A Journal of the Gesellschaft Deutscher Chemiker

Angewandte Chemie

GDCh

International Edition

www.angewandte.org

Accepted Article

Title: Fractal Crystals: Hunting the Hidden Dimension in Nanoporous Materials

Authors: Lei Wang, Shengcai Zhu, Meikun Shen, Haiwen Tian, Songhai Xie, Hongbin Zhang, Yahong Zhang, and Yi Tang

To be cited as: *Angew. Chem. Int. Ed.* 10.1002/anie.201704499
Angew. Chem. 10.1002/ange.201704499

Link to VoR: http://dx.doi.org/10.1002/anie.201704499
http://dx.doi.org/10.1002/ange.201704499

WILEY-VCH

10.1002/anie.201704499

WILEY-VCH

COMMUNICATION

Fractal Crystals: Hunting the Hidden Dimension in Nanoporous Materials

Lei Wang, [a] Sheng-cai Zhu, [b] Mei-kun Shen, [a] Hai-wen Tian, [a] Song-hai Xie, [a] Hong-bin Zhang, [a] Ya-hong Zhang[a] and Yi Tang*[a]

Abstract: Screw dislocation structure in crystal are origin of symmetry breaking in a wide range of dense phase crystals. Preparation of such analogous structure in framework phase crystals is of great importance in zeolites but still a challenge. On the basis of crystal structure-solving and model building, we found that the two specific intergrowths in MTW zeolite produce this complex fractal and spiral structure. With the structure determined parameters (spiral pitch h, screw angle θ and spatial angle ψ) of Burgers circuit, the screw dislocation structure can be constructed by two different dimensional intergrowth sections. Thus the reported complexity of various dimensions in diverse crystals can be unified.

In the prosperous field of nanoscience, a major challenge is to fabricate intricate mesostructured crystalline materials with desired architecture, morphology and dimensions. Among fascinated phenomena in nature, fractal and spiral structures have been the evergreen topics in the fields from crystallography to material science for their intriguing contributions on both fundamental researches and practical applications. The natural world we live in teems with a plenty of branching structures (e.g., snowflake, tree and galaxy). The recursive division of branches in the networks is treated as a self-similarity in fractal geometry. Additionally, the branching patterns are assembled by these fractal structures following self-similar law. On the other hand, the pivot to form spiral structure of crystal lies in the generation of screw dislocation to break the symmetry of crystal growth and promote the anisotropic nanostructures. Such dislocation structure has been widely captured in dense phase materials, such as metal oxides and alloy compounds [1], ceramics [2], carbon nanotubes [3], and even ice [4].

Comparatively, in framework materials, the complex dimension can be captured individually: i) hierarchal architecture formed by self-repeating pillared MFI [5] or rational intergrowth of FAU nanosheets [6], and ii) spiral structure in which spiral contour can be observed on the flat surface of various crystals, for instances, LTA, STA-7 (SAV), CHA/AEI, $ZnPO_4$-Sodalite and $ZnPO_4$-Faujasite. In fact, although the screw dislocation core structure was predicted in atomic scale of LTA zeolite by Walker and coworkers [7], the real ones of these frameworks remain elusive. Importantly, the high symmetry of these framework materials make the screw structure easy to be fused, leading screw dislocation structure to be embedded in the bulky crystal. MTW zeolite is known for its catalytic properties as a useful solid-acid catalyst [8]. MTW zeolite composes of “butterfly building units ($5^4 6^1$)” layers, and the butterfly building layers stack into a 3D framework along a-axis by sharing four member ring structure. It often exists as intergrown polymorphs of two end-members of monoclinic (stacking sequence: ABCABC, *C2/c*, a=24.86 Å, b=5.01 Å, c=24.33 Å, β=107.7°) and orthorhombic phase (stacking sequence: ABABAB, *Pmcn*, a=24.30 Å, b=23.70 Å, c=5.01 Å). Remarkably, some other twining behaviors, e. g., hexagonal star shape [9], are also found apart from this polymorph twinning, but the origin still remains elusive. Herein, we successfully solve crystal boundary in the branching hexagonal star of MTW zeolite with full connectivity, which is crucial in directing the evolution of regular morphology of hexagonal star. By the combination of two intergrowth along <310> and <100> directions, the unique screw dislocation core structure can be achieved by above collaborative growth behaviors in two different dimensions. Thanks to the one dimensional channel system of zeolite MTW, the unique pore direction can be adopted as dimensional indicator. Due to the lower symmetry of MTW framework, the segments around the screw dislocation cannot fuse into a bulky crystal for structure mismatching, which is different from that in the higher symmetry system (LTA, CHA/AEI, etc.). In addition, the phenomena in the framework materials with different symmetries can be unified and interpreted by the following conceptual structure.

In a typical synthesis, the reaction was performed by hydrothermal method with a diquaternary ammonium type organic structure-directing agent (OSDA) $C_4H_8(CH_3)N^+$-C_5H_{10}-$N^+(CH_3)C_4H_8$ (abbreviated as 1,5-MPP, hereafter, Figure S1, S2) containing siliceous gel. And then different type and concentration of aluminum or boron sources was selectively added into the above gel to control the supersaturation level of the system. Once homogenous gel formed, it was transferred into a Teflon-lined autoclave and hydrothermally treated at 433 K for 3 days under autogenous pressure statically. As exhibited in Figure 1, the crystallization of MTW zeolite can be divided into three regimes in its phase diagram referring to evolution of crystal structure and morphology (Figure S3-S6 and Table S1): hexagonal shape plate (Phase I, Si-Al system), numerous nanorods with layer by layer and branching mode (Phase II, Si-B system), and dendritic growth with frequently branching and stacking faults to form a spiral plate (Phase III, Si-B system).

[a] L. Wang, M. Shen, H. Tian, S. Xie, H. Zhang, Prof. Y. Zhang, Prof. Y. Tang
Department of Chemistry, Shanghai Key Laboratory of Molecular Catalysis and Innovative Materials, Laboratory of Advanced Materials, and Collaborative Innovation Centre of Chemistry for Energy Materials
Fudan University
Handan Rd. 220, Shanghai 200433 (P. R. China)
E-mail: yitang@fudan.edu.cn
[b] S. Zhu
Center for High Pressure Science and Technology Advanced Research (HPSTAR)
Shanghai 201203 (P. R. China)

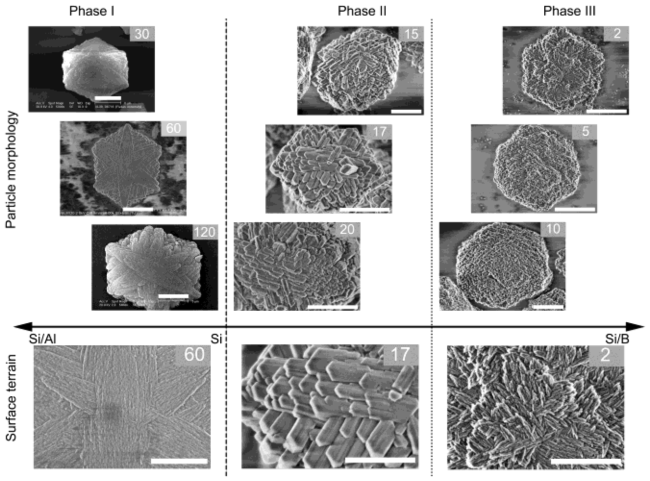

Figure 1. Evolution diagram of zeolite MTW under different supersaturation. Up: Phase I: branching growth (Si-Al system, SAR: 30-120, scale bar: 5, 2 and 5 μm), Phase II: layer by layer and branching growth (Si-B system, SBR: 20-15, medium supersaturation, scale bar: 1, 1 and 1 μm), and Phase III: dendritic growth (Si-B system, SBR:10-2, high supersaturation, scale bar: 1, 2 and 2 μm). Down: Enlarged view of MTW particles in corresponding phase diagram (scale bar: 2, 0.5 and 1 μm).

Phase I: For the zeolites synthesized in aluminosliceous system (Figure 1), the MTW zeolite is collected when Si/Al ratio in starting gel is higher than 30. The obtained samples mainly present the pseudo-hexagonal morphology composed of monoclinic phase of MTW zeolite via Rietveld refinement and related physicochemical analysis (Figure 2a, Figure S7-S9, Table S2, S3). From the TEM image (Figure 2b), one can see all particles follow a relative fixed geometry composed of one major and two minor spindle-like prisms with the angular relations of ca. 65° between major and minor branches and ca. 50° for two adjacent minor branches. During the crystallization (Figure S10, S11), the major prism forms prior to the minor ones, which can be proven in a dilute system (Figure S12). As suggested by electron diffraction (ED) patterns (Figure S13, Table S4), each prism in the crystal plate extends along its microchannel ([010] direction) and intersects to the adjacent one by sharing (*hk*0) twinning plane. Focused ion beam (FIB) dual beam experiment (Figure S14, S15) is employed to acquire the interested central thin slice in the hexagonal plate with twinning intersection. The spatial analysis in TEM-EDS experiment on the twinning slice indicates that there is no remarkable elemental difference between the domains and twinning boundaries (Figure S16, Table S5). In the low magnification TEM image, the twinning boundary of major and minor branches can be easily discerned by different textures (Figure 2c). The ED patterns of different areas exhibit increasing complexity: from Region I (the area of single main trunk) to II (that upon the intersection of the main trunk and a minor intergrown branch) and III (that upon two intersections of the main trunk and two minor intergrown branches). Firstly, in the ED pattern of the main branch locate at Region I, only a sharp dots from the [001] can be obtained (Figure 2c-I). While in ED pattern at Region II, apart from the original set of sharp dots of main trunk, another set of diffraction dots is imposed from the same [001] zone axis but with a rotation angle about 65°, implying that two sets of ED spots overlap along [310], i.e., the two adjacent branches intergrow along the specific plane. With respect to the newly formed boundary along the [310], the ED pattern of Region II exists a 180° rotation around (310) plane normal (Figure 2c-II). Interestingly, the ED pattern acquired at Region III displays the diffraction dots of all of three individual trunk/branches from [001] (Figure 2c-III). Different from the second branch, the third one intergrow to the main trunk along [3-10]. Based on anisotropic growth of MTW crystal (Figure S17), a plausible model can be constructed for pseudo-hexagonal plate with one main trunk and two minor twinning branches sharing a common *c*-axis (Figure 2d, Figure S18, S19), whose simulated ED patterns (fig S18 and S20) are in line with experimental results (Figure 2I, 2II, 2III). Its local structure of interface (Figure 2e, 2f and Figure S21) shows full atomic connectivity with the 67.9° in (the same as Figure 2b) and 20.3° out of *ab* plane. If in the concentrated system, more complex dendritic morphology with snowflake-like fractal structure of at least two generations can be clearly identified (Figure S22), where each branch was interconnected via {310} facets with a common intersection angle of ca.~65°.

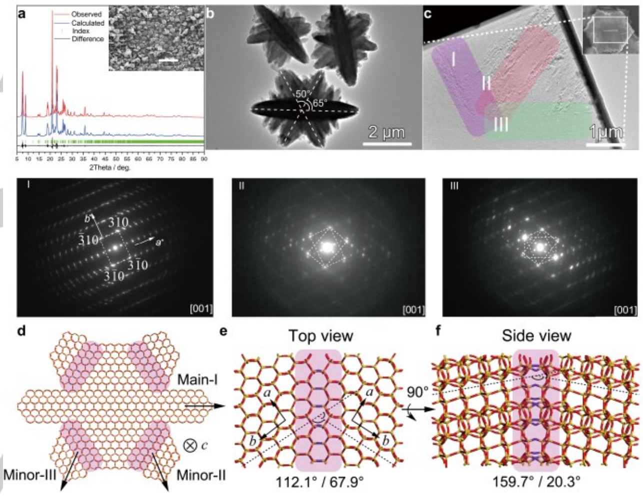

Figure 2. Morphology and twinning texture of hexagonal MTW plate. a) Rietveld refinement analysis of MTW twinning structure, R_{wp}: 7.54%, R_{wp}(w/o bck): 9.06%, R_p: 5.44%, χ^2: 1.92, (inset: representative morphology of twinning MTW plate, scale bar: 50 μm). b) Typical TEM image of hexagonal star composed of three branches with geometry 4×65°+2×50°. c) Cross-section slice of hexagonal plate, three individual branches are highlighted by different colours (inset: original hexagonal plate). Electron diffraction patterns of twinning boundaries locate at I, II and III. d) Atomistic projection model of hexagonal star with highlighted twinning boundary (arrows indicate the 1D-12MR channel system, view along *c*-axis). e-f) Atomic connectivity profiles of twinning boundary (top and aspect view), respectively.

Phase II: By screening the synthesis conditions, MTW fine structure can be deliberately control via partial substitution of T atom with boron (Figure 1, Figure S23, S24). It should be noted that, the as-synthesized zeolite displays the same hexagonal habitus (Figure S25). When SBR > 10 in which the system would locate in the medium supersaturation, MTW crystals exhibit the hexagonal plate morphology with layer-by-layer stacking crystalline branches at higher temperature for longer time (Figure S26). These rod-like branches become thinner and their stacking mode become denser with the increasement of boron content (Figure S27). The phenomena could be anticipated by Burton-Cabrera-Frank (BCF) theorem [10], in which the crystal growth is

10.1002/anie.201704499

governed by mechanisms of dislocation growth, layer-by-layer growth and fractal growth as increasing supersaturation (Figure S28).

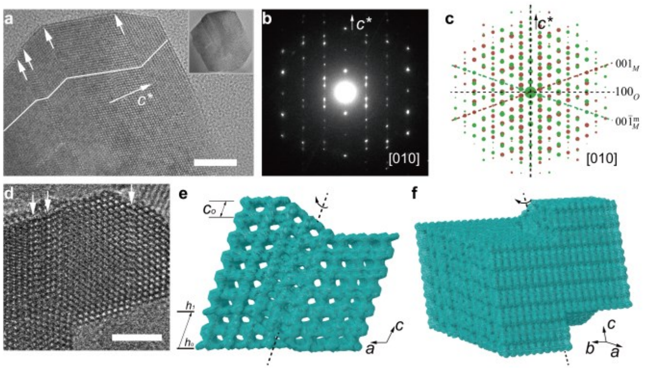

Figure 3. Stacking faults in MTW and related screw dislocation core structure. a) HRTEM image of the thin slice, arrows indicate the SFs position and the trace line presents the crystal growth direction (scale bar: 20 nm, inset: the intact cutting slice, thickness: ~ 40 nm). b) Rotated ED pattern of intact thin slice in inset of Figure 3a. c) Reconstructed ED pattern, and the dash lines mark principal direction for monoclinic phase along the [010] zone axis. d) HRTEM image of screw dislocation structures, arrows marks the fuzzy area resulted from superimposition of bilayer with different SFs, scale bar: 10 nm. e-f) Rendered 3D atomistic model of screw dislocation core (C_0: unit parameters along c-axis, h: spiral pitch, detailed atomistic framework scheme is deposited in Figure S42).

Furthermore, more detailed structure in each branch could be discerned in the HRTEM image of a microtombed slice cut from hexagonal MTW zeolite plate (SBR=17, Figure 3a). The branch has the regular hexagonal shape (Figure 3a, inset), and the stacking faults (SFs) can frequently appear along the c^* direction (Figure S29). And the ED pattern (Figure 3b) indicates that the structure is viewed along [010]. According to the MTW framework, the SFs in the crystals can be attributed to the intergrowth of monoclinic structure with mirror or two-fold operation perpendicular to c-axis via an intrinsic twining plane with orthorhombic symmetry and re-aligning to (100) plane (Figure S30, Table S6, S7). Such structure can be proved by consistence of the experimental ED pattern (Figure 3b, taken from the well-ordered microtomed thin slice in Figure 3a) and the reconstructed one (Figure 3c) from [010] zone axis of MTW zeolite. The frequent occurrence of SFs along the a-axis results in the diffuse streaks when $h \neq 3n$, while the sharp spots can be observed along the $[010]_{mono}$ when $h=3n$ (n, integer number). The phenomena indicate that the intrinsic stacking disorder derives from original monoclinic framework and presents the layer shears of $\pm 1/3a$ [11]. As indicated by structure simulation and electron diffraction, the frequent stacking disorders lead to the appearance of thin layers with orthorhombic symmetry between the monoclinic MTW domains (Figure S31, S32). For the complex crystallization process of zeolites, the layer by layer stacking structures may derive from multiple pathways of crystal growth involving the oriented aggregation between different crystal domains of MTW [12].

Phase III: When the crystallization system is turned into a high supersaturation status (SBR<10), different from those in Phase I (Figure 2 and 4a) and II (Figure 3 and 4b) with lower supersaturation, the final plates become a spiral, dendritic structure with main phase of boron-substituted monoclinic MTW (Figure 4c, S33-S39). Combining the SEM and TEM patterns (Figure S39-S41), the hyper-branching and racemic features can be easily captured. From the further inspection on the HRTEM images along channel direction, the sample exhibits a severely stacking disorder of numerous domains (Figure S42). Figures 3e and 3f show the rendered screw dislocation structure of two crystalline layers with different stacking sequences, which derives from the HRTEM results (Figure S42). Interestingly, one can see the layer by layer structures of the zeolite domains along channel direction and their related dim areas (Figure 3d, Figure S43).

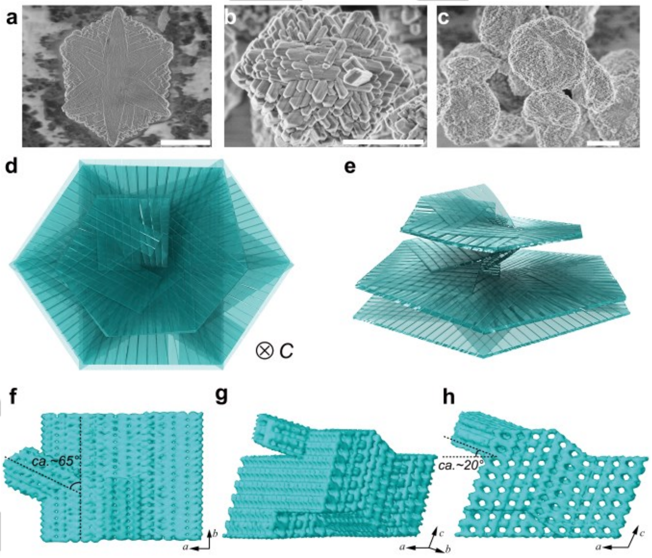

Figure 4. Collaborative growth behaviors along two different directions in MTW zeolite. a-c) Representative structure in MTW under increasing supersaturation (a: SAR=60, b: SBR=17, c: SBR=2), scale bar: 5, 1 and 2 μm, respectively. d-e) General structure of the fractal spiral structure of MTW. f-g) Rendered atomic model of the two independent growing dimensions in MTW structure observed from different directions (Detailed atomistic framework scheme is deposited in Figure S48).

The spiral, hyper-branched structure of Phase III can be recognized as the overlay of above twinning status of MTW zeolite in two different dimensions, i.e., (1) the stacking disorder in ac planes (Figure 3) and (2) the deformation twinning in ab plane (Figure 2), which construct the screw dislocation core region as the driving force to form this spiral structure in the hexagonal plate (Figure 4). On one hand, as shown in Figure 3E and 4H as example, the unique stacking disordered structure is born to break the crystal symmetry in ac plane (which can also be captured in dense crystal [1c, 1d, 2]): (i) first domain (top layer) with even numbered ($2n$; n, integer number) SFs (Figure S44, S45) and (ii) the other one (bottom layer) without SFs. The top domain with even numbered faults aligns in parallel to the bottom defect-free one in starting and ending parts due to the same stacking vector (Figure S46, S47). An intact Burgers circuits is thus formed [13] for exertion of the screw dislocation structure (Figure 3e, 3f) with a regular spiral pitch $h=nC_0$ (n, integer number; C_0, 1/2 unit parameters along c-axis). On the other hand, the deformation twinning at (310) plane leads the generation of the branches with screw angle (θ) of 67.9° in ab plane and spatial angle (ψ) of 20.3° out of ab plane (Figure 4f-4h) referred to results in Figure 2. These two factors are the structural foundation of the spiral, hyper-branched structure of Phase III, and the collaborative growth behavior in two dimensions generates fractal spiral structure. With

10.1002/anie.201704499

increasement of boron content, the prisms in the hexagonal plate particles appear more frequently with smaller size to form a dendritic pine tree-like branches in *ab* plane. Furthermore, the frequently 2-D nucleation events on the plates bring about the frequent appearance of SFs along *a*-axis (looking down *ac* plane) to form the screw dislocation core region with numerous fragments (Figure S48), which further promotes fractal growth in *ab* plane by fast extension along the channel direction and facilitates the continuous self-iteration process.

Such screw dislocation structure creates inner strain (E_{strain}) in the periodic crystalline lattice. According to the elastic theory, the stress field exerts a torque throughout the whole plate at the central area, and the strain energy depends on the magnitude $E_{strain} \propto b^2$ (***b***, Burgers vector). The phenomena were often observed in dislocation-driven dense phase materials, such as ZnO nanotubes or Bi_2Se_3 plates [1c, 1d]. An energy balance between surface energy $2\pi r\gamma$ (γ, surface energy) and inner strain E_{strain} can be spoiled, and the solid plate becomes a hollow one as be confirmed in this work (Figure S49-S51).

The above conceptual evolution model of spiral structure of MTW also can be adopt to interpret those in the nanoporous materials with different topology. For a known screw dislocation, there must be a birth in plane and a spread along vertical direction in crystal, which involves the two collaborative growth behaviors along the two different dimensions. As previously reported spirals in nanoporous systems, like LTA [7, 14] (Figure S52, Table S8), CHA/AEI [15] , STA-7 (SAV) [16], $ZnPO_4$-Sodalite and $ZnPO_4$-Faujasite [17], 3D spiral terraces are considered here to be defined by three crucial parameters: spiral pitch h, screw angle θ and spatial angle ψ. For LTA zeolite, the above two angles are 90° and 0°, respectively. In the each corner of the LTA square spiral terrace, the adjacent segments rotate about 90° and fuse into the bulky crystal owing to the identical atomic arrangement in the (010) and (001) planes. It worth noting that other nanoporous materials with high symmetric level always fuse into their bulky crystal and leave a spiral terrace on the surface due to the overlap of two dimensions, which may explain that why we seldom capture the screw dislocation structure in nanoporous system [7, 18]. In MTW zeolite with lower symmetry (*C2/c*), the three parameters are determined as spiral pitch: 1.2 nm, screw angle: 67.9° with spatial angle: 20.3°, and the layer by layer stacked branches aggregate into a pine tree-like, spiral contour on the original hexagonal plane. Different from regular spiral terrace on the flat zeolite surface, [13-16] it is hard to obtain the regular spiral step height on the highly dendritic surface structure of MTW (equal to the Burgers vector along the vertical direction) by atomic force microscopy, but the spiral patterns and hillocks can still be clearly recognized.

In summary, we proposed the conceptual structural model of MTW zeolite spiral plates driven by the screw dislocation region, which is confirmed by the features of surface spiral contours, screw dislocation core and hollow core structure. Different from nanoporous materials with high symmetry (e.g., CHA/AEI [15], SiC ceramic [2, 19]), the special growth mode in this MTW zeolite plate involves the collaborative manner of frequent intergrowth along (310) plane and propagation of SFs along the vertical dimension. The dimensional change of nano-sized zeolite rods via iterative deformation twinning and intrinsic intergrowth procedure is a novel strategy toward hierarchical materials with interconnected abundant pore structures (Figure S53-S55). This strategy might be applied to other zeolite structures that can (i) derive a novel zeolite phase by regular extension of deformation twinning boundary (Figure S56) and (ii) offer a potential opportunity to distinguish the end-polymorph from hybrid phases (Table S6, S7). Furthermore, such zeolite with confirmed complex twinning and stacking faults were proven with an enhanced catalytic performance due to its textural and framework properties (Supplementary Text, Figure S57, S58).

Additionally, the model for polymorph intergrowth in this work is totally different from the known models that developed for MFI/MEL and FAU/EMT systems. For MFI/MEL, the central MEL node with higher symmetry plays as direct connector with lower symmetrical MFI nanosheets to form self-pillared pentasil [5]. For FAU/EMT, the random EMT nuclei intergrowth with FAU nanosheets to break the cubic symmetry to form hierarchical structure [6]. The orthorhombic polymorph in the screw dislocation of MTW zeolite only acts as a bridge to change the relative position along the screw dislocation circuit, and can be manipulated by surpersaturation. The unique phenomena also provide a novel vision to understand the polymorph intergrowth and its role in the architectural evolution of zeolite. Vary from the exact fractal patterns by mathematical expressions, the fractal pattern in practice is self-similarity in statistics and evolves under certain circumstance with time. Essentially, the fractal system depends on the two crucial factors: element with self-similarity and dynamic iteration procedure. The present fractal pattern is self-organized by branching and intrinsic twinning to construct a hierarchal dissipative structure under the domination of energy.

Acknowledgements

This work was supported by National Key Basic Research Program of China (2013CB934101), and NSFC (21433002, 21573046, 21473037 and U1463206). We thank Dr. J. L. Sun (Peking University) for helpful suggestions on disordered structures and Dr. P. Guo (DICP) for thoughtful discussions. We thank G. R. Zhou for cutting thin slice of the samples for HRTEM observation. Special thanks are due to reviewers for many helpful comments.

Keywords: zeolite structure • coincidence boundary • intergrowth • structure evolution • fractal pattern

[1] a) M. J. Bierman, Y. K. A. Lau, A. V. Kvit, A. L. Schmitt, S. Jin, *Science* **2008**, *320*, 1060-1063; b) J. Zhu, H. Peng, A. F. Marshall, D. M. Barnett, W. D. Nix, Y. Cui, Nat. *Nanotechnol.* **2008**, *3*, 477-481; c) S. A. Morin, M. J. Bierman, J. Tong, S. Jin, *Science* **2010**, *328*, 476-480; d) A. Zhuang, J.-J. Li, Y.-C. Wang, X. Wen, Y. Lin, B. Xiang, X. Wang, J. Zeng, *Angew. Chem. Int. Ed.* **2014**, *53*, 6425-6429.

[2] S. Harada, Alexander, K. Seki, Y. Yamamoto, C. Zhu, Y. Yamamoto, S. Arai, J. Yamasaki, N. Tanaka, T. Ujihara, *Cryst. Growth Des.* **2012**, *12*, 3209-3214.

[3] F. Ding, A. R. Harutyunyan, B. I. Yakobson, *Proc. Natl. Acad. Sci.* **2009**, *106*, 2506-2509.

[4] K. Thuermer, S. Nie, *Proc. Natl. Acad. Sci.* **2013**, *110*, 11757-11762.

[5] a) X. Zhang, D. Liu, D. Xu, S. Asahina, K. A. Cychosz, K. V. Agrawal, Y. Al Wahedi, A. Bhan, S. Al Hashimi, O. Terasaki, M. Thommes, M. Tsapatsis, *Science* **2012**, *336*, 1684-1687; b) D. Xu, G. R. Swindlehurst, H. Wu, D. H. Olson, X. Zhang, M. Tsapatsis, *Adv. Funct. Mater.* **2014**, *24*, 201-208.

[6] M. Khaleel, A. J. Wagner, K. A. Mkhoyan, M. Tsapatsis, *Angew. Chem. Int. Ed.* **2014**, *53*, 9456-9461.

[7] A. M. Walker, B. Slater, J. D. Gale, K. Wright, *Nat. Mater.* **2004**, *3*, 715-720.

[8] W. Vermeiren, J.-P. Gilson, *Top. Catal.* **2009**, *52*, 1131-1161.

[9] a) S. Ritsch, N. Ohnishi, T. Ohsuna, K. Hiraga, O. Terasaki, Y. Kubota, Y. Sugi, *Chem. Mater.* **1998**, *10*, 3958-3965; b) I. Kinski, P. Daniels, C. Deroche, B. Marler, H. Gies, *Microporous Mesoporous Mater.* **2002**, *56*, 11-25.

[10] a) W. K. Burton, N. Cabrera, F. C. Frank, *Philos. Trans. R. Soc., A* **1951**, *243*, 299-358; b) in *Crystal Growth for Beginners*, 2nd ed., World Scientific, **2011**, pp. 1-75.

[11] a) M. Moliner, J. González, M. T. Portilla, T. Willhammar, F. Rey, F. J. Llopis, X. Zou, A. Corma, *J. Am. Chem. Soc.* **2011**, *133*, 9497-9505; b) T. Willhammar, J. Sun, W. Wan, P. Oleynikov, D. Zhang, X. Zou, M. Moliner, J. Gonzalez, C. Martínez, F. Rey, A. Corma, *Nat. Chem.* **2012**, *4*, 188-194.

[12] J. J. De Yoreo, P. U. P. A. Gilbert, N. A. J. M. Sommerdijk, R. L. Penn, S. Whitelam, D. Joester, H. Zhang, J. D. Rimer, A. Navrotsky, J. F. Banfield, A. F. Wallace, F. M. Michel, F. C. Meldrum, H. Cölfen, P. M. Dove, *Science* **2015**, *349*.

[13] R. L. Penn, J. F. Banfield, *Science* **1998**, *281*, 969-971.

[14] S. Dumrul, S. Bazzana, J. Warzywoda, R. R. Biederman, A. Sacco Jr, *Microporous Mesoporous Mater.* **2002**, *54*, 79-88.

[15] R. L. Smith, W. A. Slawinski, A. Lind, D. S. Wragg, J. H. Cavka, B. Arstad, H. Fjellvag, M. P. Attfield, D. Akporiaye, M. W. Anderson, *Chem. Mater.* **2015**, *27*, 4205-4215.

[16] P. Cubillas, M. Castro, K. E. Jelfs, A. J. W. Lobo, B. Slater, D. W. Lewis, P. A. Wright, S. M. Stevens, M. W. Anderson, *Cryst. Growth Des.* **2009**, *9*, 4041-4050.

[17] P. Cubillas, M. W. Anderson, in *Zeolites and Catalysis*, Wiley-VCH Verlag GmbH & Co. KGaA, **2010**, pp. 1-55.

[18] R. L. Smith, A. Lind, D. Akporiaye, M. P. Attfield, M. W. Anderson, *Chem. Commun.* **2015**, *51*, 6218-6221.

[19] J. Hassan, J. P. Bergman, A. Henry, E. Janzén, *J. Cryst. Growth* **2008**, *310*, 4424-4429.

10.1002/anie.201704499

Entry for the Table of Contents (Please choose one layout)

Layout 2:

COMMUNICATION

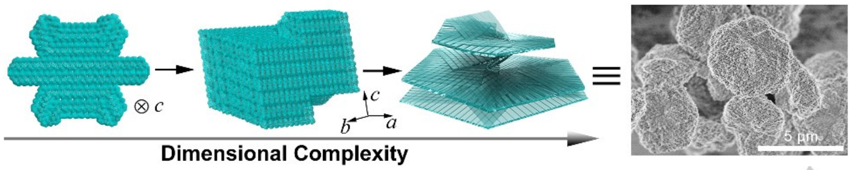

*L. Wang, S. Zhu, M. Shen, H. Tian, S. Xie, H. Zhang, Y. Zhang and Y. Tang**

Page No. – Page No.

Fractal Crystals: Hunting the Hidden Dimension in Nanoporous Materials

Hunting the hidden dimension in nanoporous materials! Revealing that experimental screw dislocation structure in MTW zeolite is constructed by two specific rational intergrowth along different dimensions.